Sta 440 Case 4

Christina Lee, Steph Reinke

2025-11-01

1. Background

Root growth in the rice plant is characterized by a distinct rotational motion called circumnutation. Researchers want to better understand this process. Experimental data was collected on the developing roots of two strains of rice plants, one a wild type (WT) variety and the other a mutant (MU) variety that lacks circumnutation. In particular, cell length and position measurements were collected on cells on the inner and outer curves of a sample of roots representing the two genetic strains. The protocol utilized in this study is as follows:

1. The mid–line on the central slice of a root and its point of maximum curvature are identified
2. The lengths of the cells on the inner and outer curves of the root slice are measured and recorded for those cells falling in a window around the point of maximum curvature.

This process was repeated on nine WT and eleven MU genotype roots. By understanding the differences in growth based on side and genotype, researchers can gain a better understanding of circumnutation and rice plants.

Research Questions

Can the physical mechanism behind root circumnutation in the wild type plants be explained by differential patterns of cell growth on opposing sides of the root? Is there evidence that these patterns are diminished in the mutant genotype?

2. Data and Frequentist Model

To answer these questions we examined the resulting dataset of the process described above. The dataset contains: length, midline (distance from root tip along midline), root ID ((WT)1-9 $ (MU)1-11), side (inner or outer), and genotype (wild type (WT) & mutant (MU)) for each observation. We conducted exploratory data analysis to see how length varied by root, side, and genotype. For WT roots, there is a visible difference between inner and outer cell lengths, and this difference varies by root id (Fig 1). For MU roots, the inner and outer cell lengths tend to be similar (Fig 2). A combined analysis showed that inner and outer cell lengths are distributed the same for MU roots, while outer tends to be longer than inner cells for WT roots (Fig 3).

We began with a frequentist nonlinear model to explore if Length varied by side and genotype. Our initial approach used was a seven parameter logistic curve with side and genotype effects. However, after discussion we determined that this model inappropriately assumed a constant midline across roots, which limited its biological realism. To address this issue, we refit the data using a four parameter logistic growth model with root specific random effects. The model estimates cell length (Length) as a function of scaled midline position (M):

$$\log(\text{Length}_{ij}) = L + \frac{U_{ij} - L}{1 + \exp\left(-\frac{M_{ij} - \text{xmid}_{ij}}{s_{ij}}\right)}$$

Where: L: lower asymptote (minimum log Length), U_{ij}: upper asymptote (maximum log Length) for observation i in root j, $xmid_{ij}$: midpoint (inflection point) of sigmoid curve, s_{ij}: scale parameter, M_{ij}: scaled midline position

We included fixed effects for side (inner vs outer) and genotype (WT vs MU), as well as their interaction on U and xmid to test whether growth patterns differ across genotypes and sides of the root. Random effects for xmid and s were included at the root level to allow for root specific inflection points and slopes, accounting for biological variability in growth. Because residual plots from earlier indicated heteroskedasticity we log transformed our response variable (Length) to improve model fit.

The model was fit using the nlme package in R. Convergence was achieved by extending the max iterations to 200. Residuals versus fitted values by genotype, side, and root do not show any systematic structure (Fig 4-7). The QQ plot of the residuals followed the diagonal line suggesting that normality was met (Fig 8). The predicted curves by side (outer vs inner) were plotted against the data, which showed goodness of fit. No visible difference could be seen between the two MU curves, but the outer curve had consistently larger lengths for the WT (Fig 9). The key parameters are the side and genotype interaction terms for U and xmid. The estimated coefficient for the interaction between side, genotype and U was negative, but not statistically significant (p-value of 0.5603) (Table 1). The estimated coefficient for the interaction between side, genotype, and xmid was negative and statistically significant (p-value of <0.001) (Table 1). This suggests that for WT roots the inflection point occurs closer to the root base on the outer side compared to the inner side and compared to MU roots. Thus supporting differential patterns of cell growth by side and genotype.f

3. Bayesian Model

Main model equation

$$\log(\text{Length}_{ij}) \sim \mathcal{N}(\mu_{ij}, \tau_{\text{within}})$$

$$\mu_{ij} = L + \frac{U_{ij} - L}{1 + \exp\left(-\frac{M_{ij} - \text{xmid}_{ij}}{s_{ij}}\right)}$$

Fixed Effects (same as frequentist)

Upper asymptote (U)**:**

$$U_{ij} = \beta_{U,0} + \beta_{U,\text{side}} \cdot \text{Side}_{ij} + \beta_{U,\text{geno}} \cdot \text{Genotype}_{ij} + \beta_{U,\text{side}\times\text{geno}} \cdot \text{Side}_{ij} \times \text{Genotype}_{ij}$$

Midpoint (xmid):

$$\text{xmid}_{ij} = \beta_{\text{xmid},0} + \beta_{\text{xmid,side}} \cdot \text{Side}_{ij} + \beta_{\text{xmid,geno}} \cdot \text{Genotype}_{ij} + \beta_{\text{xmid,side}\times\text{geno}} \cdot \text{Side}_{ij} \times \text{Genotype}_{ij} + b_{\text{xmid},j}$$

Scale parameter (on log scale for positivity):

$$s_{ij} = \exp(b_{s,0} + b_{s,j})$$

Random Effects Priors

$$b_{\text{xmid},j} \sim \mathcal{N}(0, \tau_{\text{xmid}})$$
$$b_{s,j} \sim \mathcal{N}(0, \tau_s)$$

Fixed Effects Priors

$$L \sim \text{Uniform}(1, 3)$$
$$\beta_{U,0} \sim \text{Uniform}(2, 4)$$
$$\beta_{U,\text{side}}, \beta_{U,\text{geno}}, \beta_{U,\text{side}\times\text{geno}} \sim \mathcal{N}(0, 10)$$
$$\beta_{\text{xmid},0} \sim \text{Uniform}(0.3, 0.7)$$
$$\beta_{\text{xmid,side}}, \beta_{\text{xmid,geno}}, \beta_{\text{xmid,side}\times\text{geno}} \sim \mathcal{N}(0, 10)$$
$$b_{s,0} \sim \mathcal{N}(\log(0.2), 1)$$

Variance Parameter Priors

$$\sigma \sim \text{Uniform}(0, 2)$$
$$\sigma_{\text{xmid}} \sim \text{Uniform}(0, 1)$$
$$\sigma_s \sim \text{Uniform}(0, 1)$$

Next, we fit a Bayesian version of our frequentist model using JAGS and MCMC sampling. Because our nonlinear growth model was complex, the dataset was relatively small (20 roots), and the data had a hierarchical structure, a Bayesian approach was beneficial to use. It allowed us to use prior knowledge about biologically reasonable parameter ranges and to obtain stable estimates through partial pooling across roots. We used the four-parameter logistic growth model to describe how cell length (after applying a log transformation) changes along the middle of the root. The model parameters represent key features of growth including the lower asymptote (L) which reflects baseline cell size near the root tip, the upper asymptote (U) which represents maximum cell length in the differentiation zone, the midpoint (xmid) which indicates where elongation is most rapid, and the scale parameter (s) which controls how steeply the transition between zones occurs. To test our main hypothesis that uneven growth between the inner and outer sides of the root causes circumnutation and that it is not present in the mutant, we included fixed effects for side, genotype, and their interaction on both the U and xmid parameters. The interaction terms directly test whether the inner-outer growth difference changes between wild-type and mutant plants. We included random effects for xmid and s (modeled on the log scale to maintain positivity) to account for variation among individual roots and within-root correlation. We also made sure to specify weakly informative priors in order to best reflect reasonable expectations in terms of biology and plants. For example, L had a Uniform(1, 3) prior, U had a Uniform(2, 4) prior to make sure mature cells are larger than the young growing cells, xmid had a Uniform(0.3, 0.7) prior to keep the midpoint within the main root region, and the log-scale parameter for s had a Normal(log(0.2), 1) prior. All side and genotype effects were given Normal(0, 10) priors, which limited extreme values but allowed effects in either direction (positive or negative). Standard deviation parameters had Uniform(0, 2) priors for observation level error and Uniform(0, 1) priors for random effect variability. In total, we ran four MCMC chains for 50,000 iterations, discarded the first 10,000 as burn-in, and retained every 10th sample, which resulted in 16,000 posterior samples.

The Bayesian hierarchical model showed good convergence and fit to the data. For example, the MCMC trace plots showed good mixing across all four chains, and the Gelman-Rubin statistics were near 1.0 for all

parameters (Table 2). Effective sample sizes for all key parameters exceeded 1,300, and most of the random effects achieved ESS values between 3,000 and 8,000 (Table 3). This shows that there was sufficient posterior sampling. Furthermore, the fitted curves of the Wild Type Roots (Fig 13) show that the model accurately captured the sigmoidal growth pattern in all nine wild-type roots. They also show a clear separation between inner (red) and outer (blue) curves, which adds to supporting the differential growth based on our research question. The residual tests (Fig 14) show that the model assumptions were met. This includes how the residuals were approximately normally distributed according to the Normal Q-Q plot, no systematic patterns being present across the fitted values or scaled midline position, and consistent variance being present across the genotypes and sides (Fig 15). Additionally, the posterior density plots (Fig 16) provided strong evidence supporting the gravitropism hypothesis. The density for the side_effect_WT_U parameter was positive and clearly separated from zero, which indicates that the wild-type roots showed a big enough differential growth, where the outer cells reached greater maximum lengths than inner cells. In contrast, the density for side_effect_MU_U was centered near zero with greater overlap, which shows that there was minimal differential growth in the mutant roots. The density for interaction_xmid showed a negative peak, which indicates that the midpoint of elongation occurred earlier on the outer side in wild-type roots compared to mutants, which is consistent with the asymmetric developmental timing mentioned in the background. The trace plots (Fig 11 & 12) for these parameters indicated stable chains with no signs of non-convergence or autocorrelation, which supports the posterior estimates. Overall, these results provide strong Bayesian evidence that differential cell elongation between the inner and outer sides of the root is emphasized in wild-type plants and reduced in the mutant genotype. This supports the conclusion that differential growth driven by gravitropism is a key feature underlying root circumnutation in rice plants.

4. Shortcomings and Assumptions

There were several important limitations and assumptions regarding our insights. The first is that the sample size was relatively small with only 20 root types. This limits statistical power and increases uncertainty around parameter estimates. This is particularly an issue with MU roots, where between root variability was higher. Another limitation is that the frequentist model we chose may have oversimplified the data. A four parameter logistic curve may oversimplify the true biological process of root growth because it assumes smooth, systematic growth along the midline. We assumed that U and L did not vary significantly across roots, which may not reflect reality. Lastly the priors that we chose for our Bayesian model were not chosen through a formal sensitivity analysis. Even though we chose weakly informative priors, they could still have constrained parameters beyond bounds seen in reality.

Both modeling frameworks assume that the residuals are approximately normal with constant variance. Normality was met in both models, with QQ plots that followed the diagonal line (Fig 8). Residuals for our frequentist model were randomly scattered when examined all together and by side, root, and genotype (Fig 4-7). There were slight variances in range for differing roots, but all individual roots roughly followed a random scatter with roughly constant variance. Overall the residuals tended to be more concentrated at lower fitted values. This effect was more prominent in the MU roots than the WT roots.

5. Conclusion

Across both frequentist and Bayesian frameworks, we found consistent evidence that wild-type (WT) roots exhibit significant asymmetry in cell elongation, while mutant (MU) roots do not. The frequentist nonlinear mixed-effects model revealed that the inflection point (xmid) occurred significantly closer to the root base on the outer side for WT roots, suggesting earlier elongation onset relative to the inner side. In contrast, MU roots showed no such difference. The Bayesian hierarchical model corroborated these findings, providing strong posterior support that outer-side cells in WT roots achieved larger maximum lengths (U) and earlier elongation midpoints (xmid) than inner-side cells, consistent with asymmetric growth driving circumnutation.

Together, these findings suggest that differential elongation across root sides is a defining feature of wild-type root development and likely represents the physical mechanism underlying circumnutation. The absence of

such asymmetry in mutant roots reinforces the hypothesis that the genetic mutation disrupts the gravitropic signaling or growth response necessary for this motion.

6. Appendix

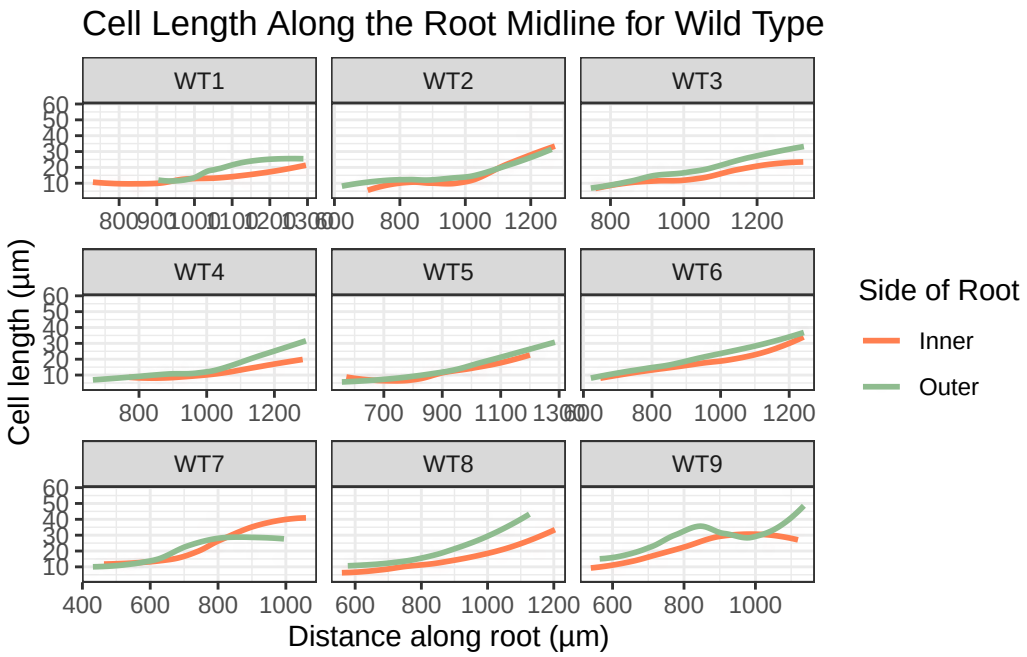

Figure 1: The difference between inner and outer cell lengths changes root by root

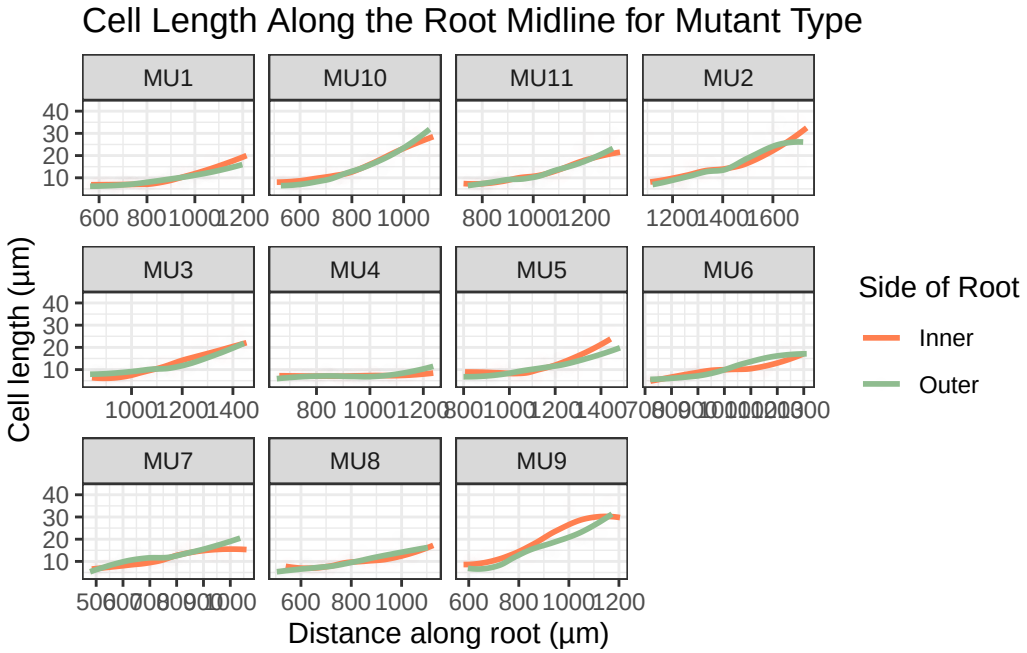

Figure 2: There is only slight differences between inner and outer cell lengths

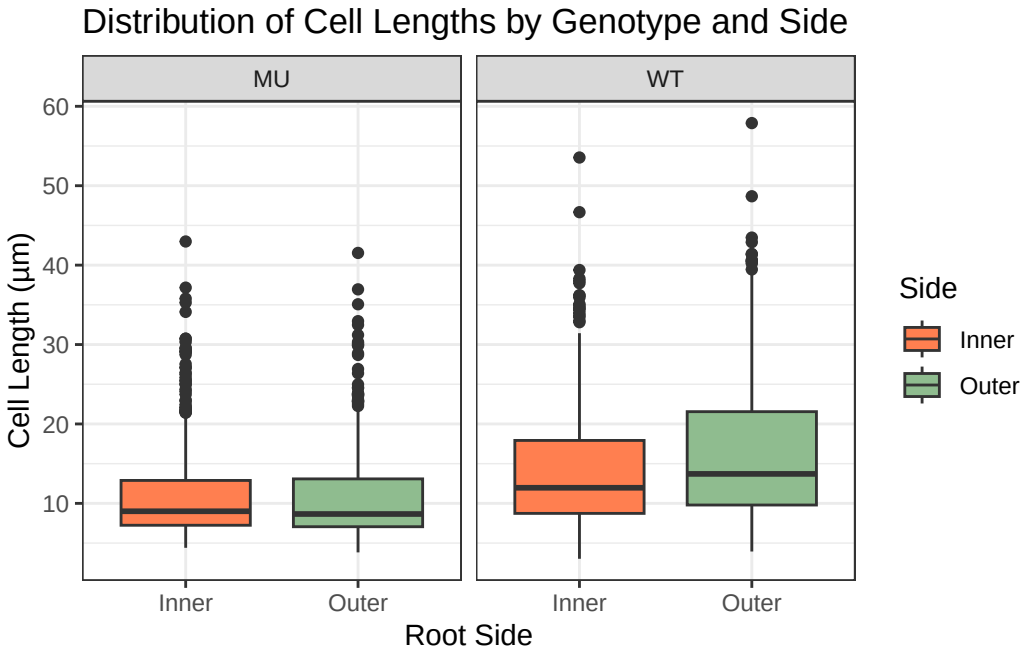

Figure 3: MU cells have similar inner vs outer lengths; WT outer has longer lengths than inner

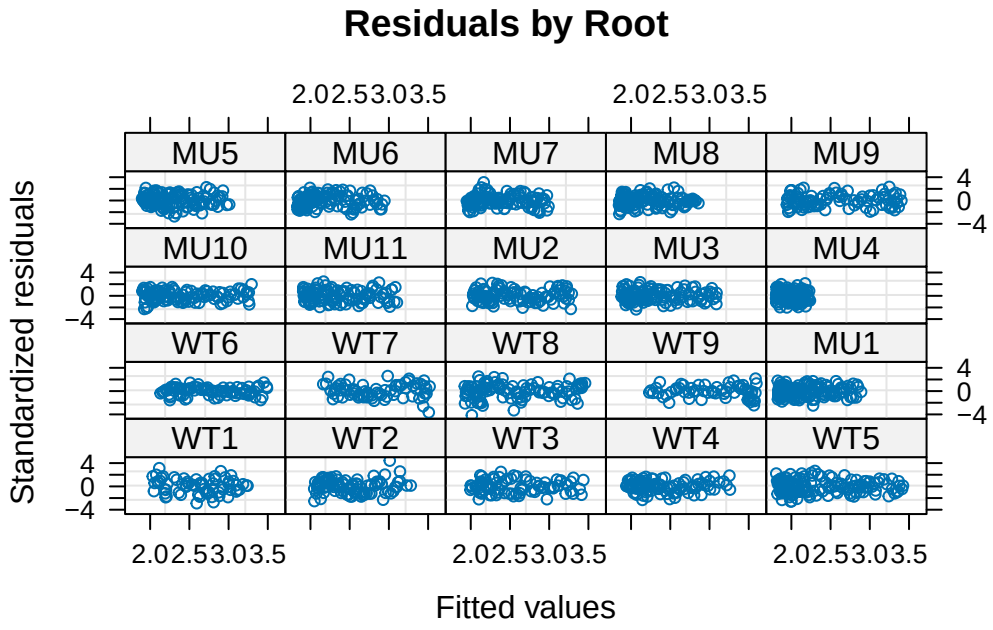

Figure 4: Residual plot by root id shows variation by root with better scatters for WT

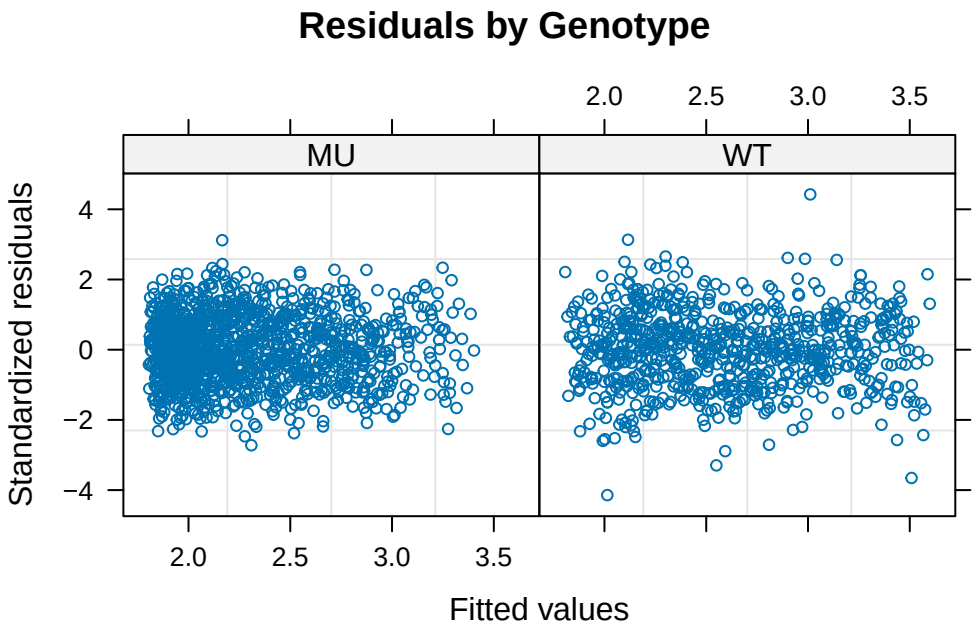

Figure 5: Residuals by Genotype show random scatter and constant variance, MU more dense at lower values

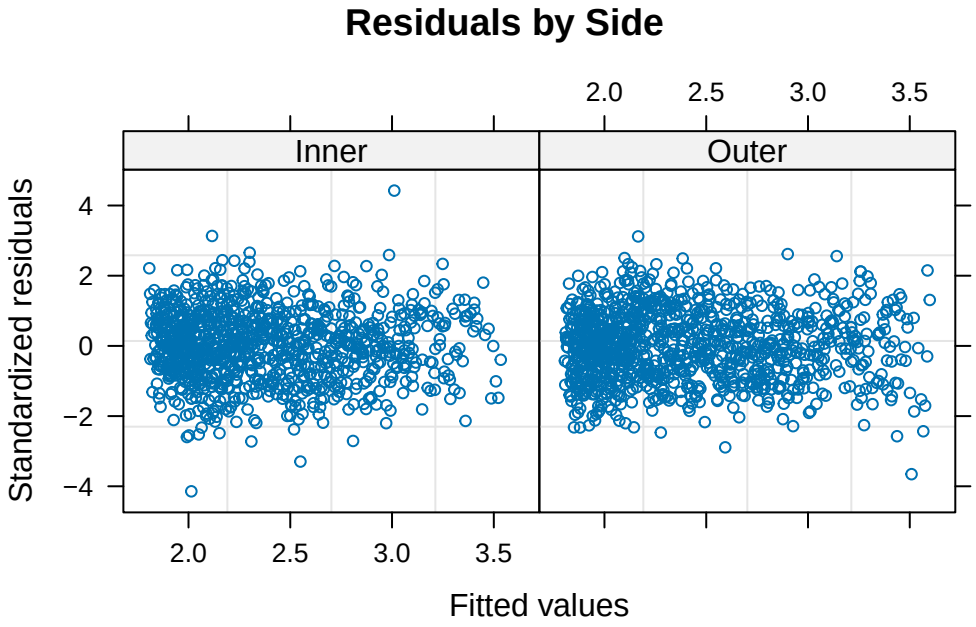

Figure 6: Residuals by Side show random scatter and constant variance more dense at lower values

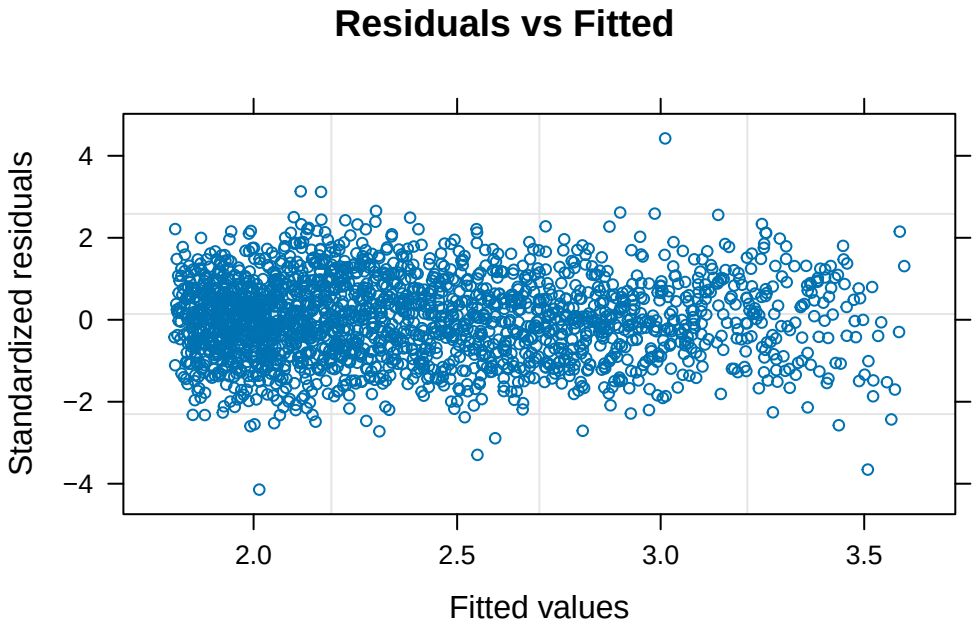

Figure 7: Residual plot for all data shows random scatter and constant variance, more dense at lower values

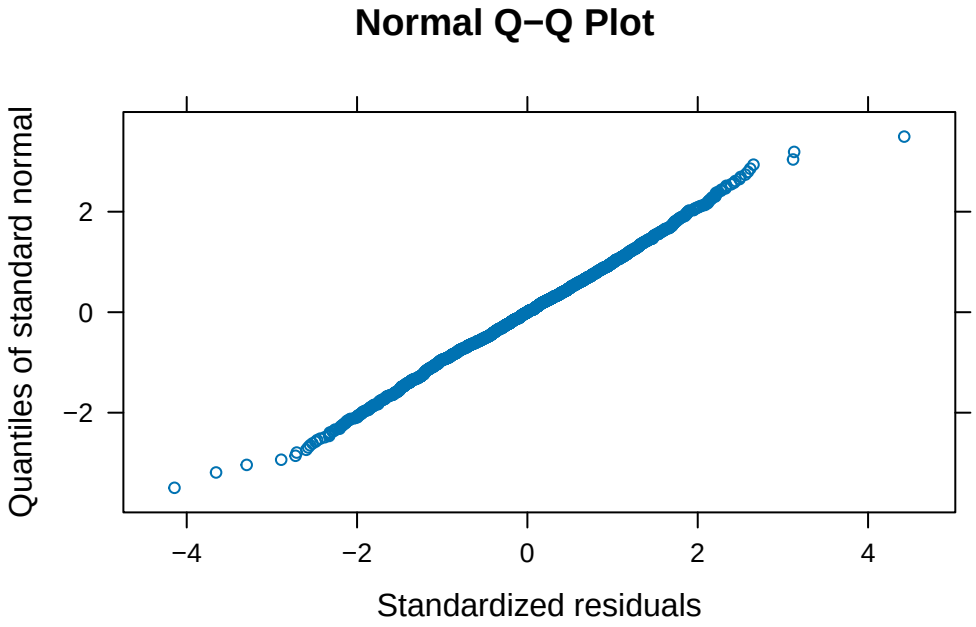

Figure 8: QQ plot shows residuals follow diagnol line, shows normality

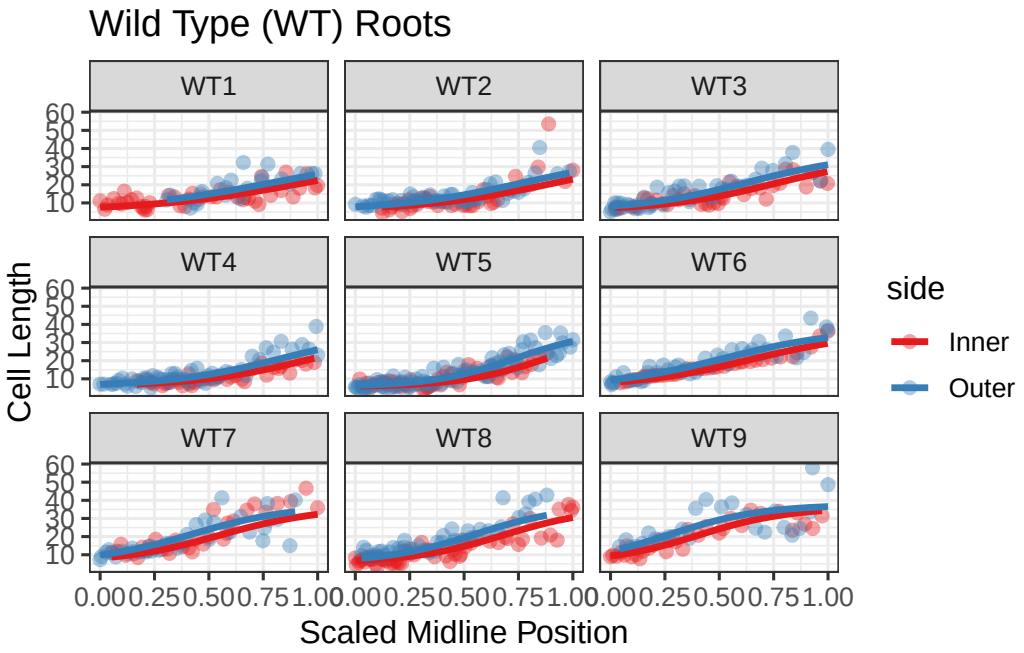

Figure 9: Data vs fitted curves shows goodness of fit for WT

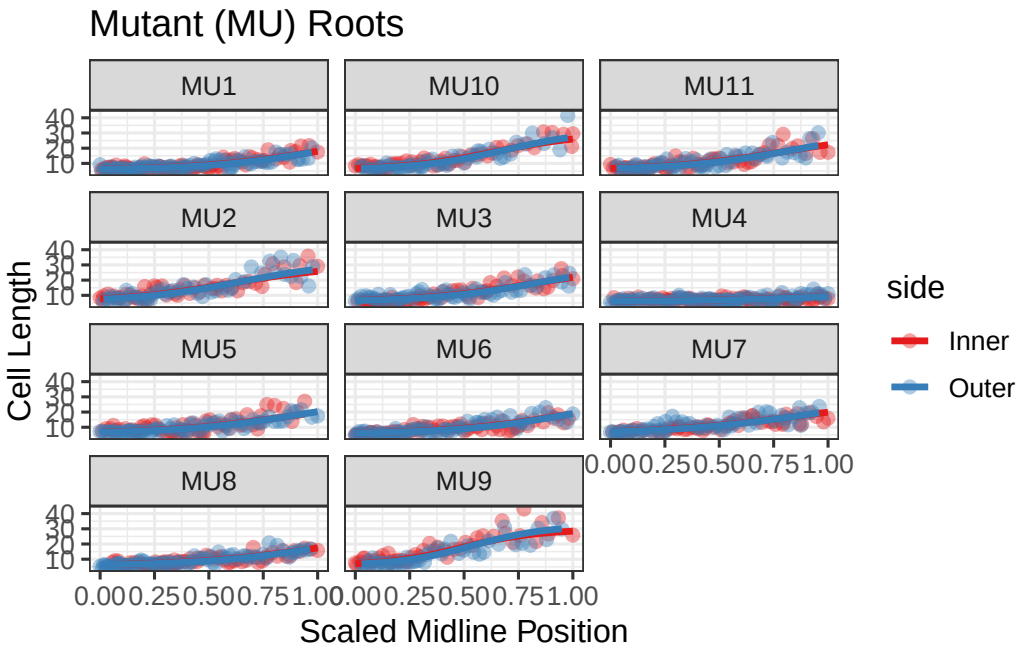

Figure 10: Data vs fitted curves shows goodness of fit for MU

Table 1: Model output for frequentist model

	Value	Std.Error	DF	t-value	p-value
L	1.7376245	0.0318986	2077	54.4734396	0.0000000
U.(Intercept)	3.3913224	0.0716386	2077	47.3393166	0.0000000
U.sideOuter	0.0886904	0.0690895	2077	1.2837020	0.1993894

	Value	Std.Error	DF	t-value	p-value
U.GenotypeWT	0.2004287	0.0899438	2077	2.2283765	0.0259621
U.sideOuter:GenotypeWT	-0.0531306	0.0912027	2077	-0.5825553	0.5602559
xmid.(Intercept)	0.6468256	0.0641757	2077	10.0789831	0.0000000
xmid.sideOuter	0.0455478	0.0233569	2077	1.9500751	0.0513015
xmid.GenotypeWT	-0.1064539	0.0764380	2077	-1.3926832	0.1638647
xmid.sideOuter:GenotypeWT	-0.1750729	0.0317632	2077	-5.5118061	0.0000000
s	0.2777700	0.0213874	2077	12.9875252	0.0000000

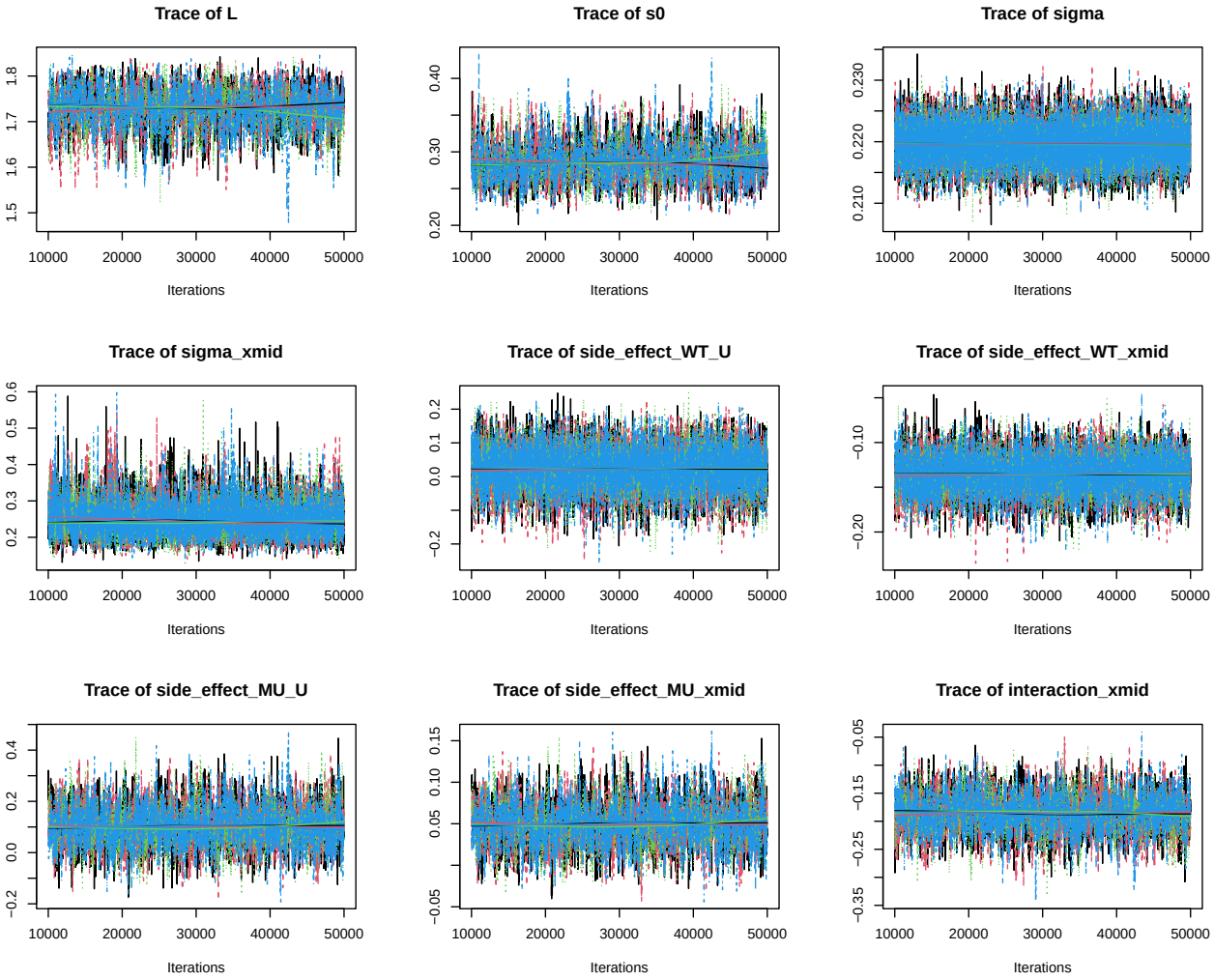

Figure 11: Trace plots for main parameters

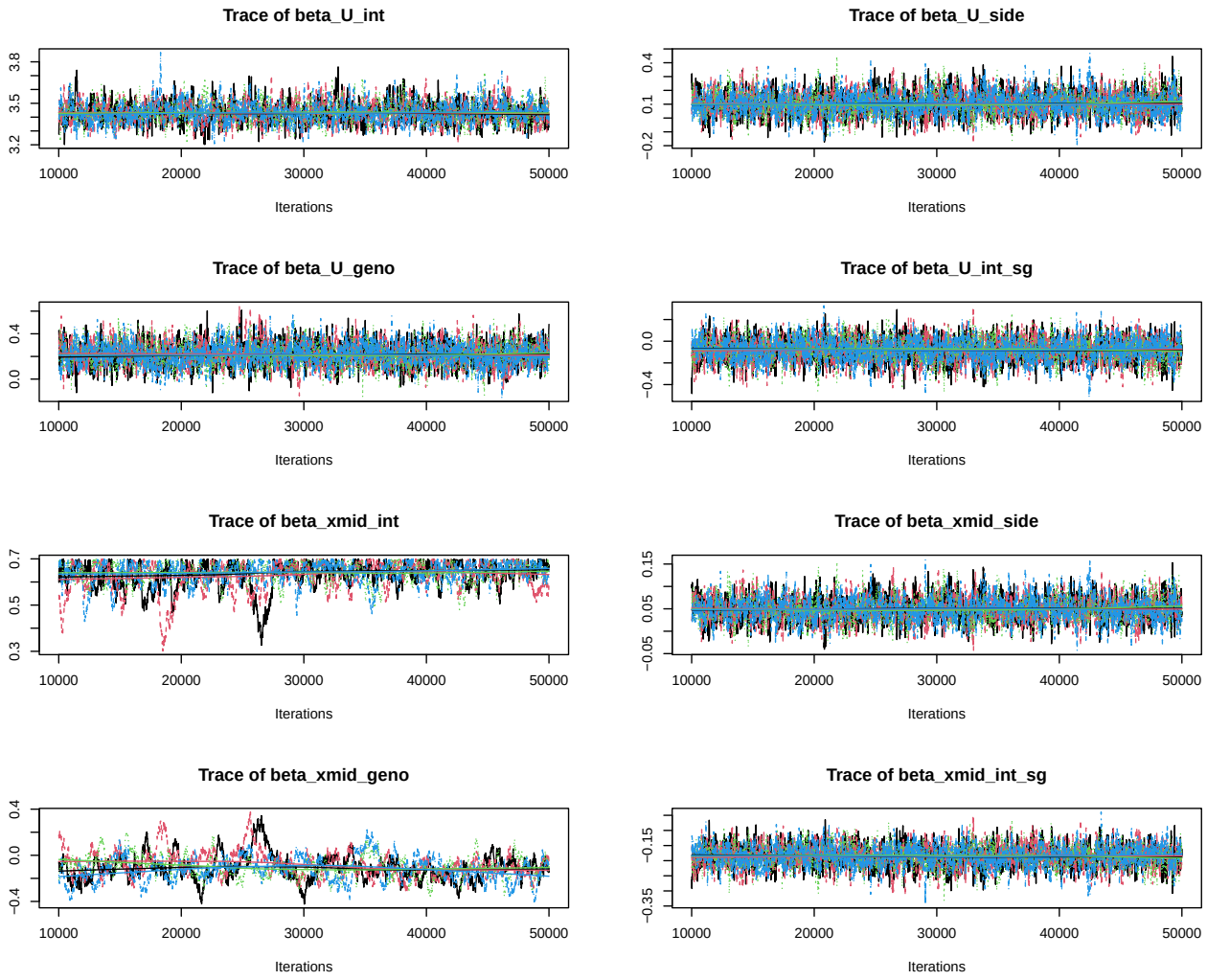

Figure 12: Trace plots for beta parameters

Table 2: Gelman-Rubin convergence diagnostics for main parameters

	Point est.	Upper C.I.
b_s[1]	1.000	1.000
b_s[10]	1.000	1.001
b_s[11]	1.000	1.001
b_s[12]	1.000	1.000
b_s[13]	1.000	1.001
b_s[14]	1.000	1.000
b_s[15]	1.003	1.009
b_s[16]	1.000	1.000
b_s[17]	1.000	1.001
b_s[18]	1.000	1.001
b_s[19]	1.000	1.001
b_s[2]	1.001	1.002
b_s[20]	1.000	1.001
b_s[3]	1.000	1.001
b_s[4]	1.000	1.000

	Point est.	Upper C.I.
b_s[5]	1.000	1.000
b_s[6]	1.001	1.003
b_s[7]	1.000	1.001
b_s[8]	1.002	1.004
b_s[9]	1.000	1.001
b_s0	1.002	1.007
b_xmid[1]	1.005	1.014
b_xmid[10]	1.014	1.022
b_xmid[11]	1.014	1.022
b_xmid[12]	1.014	1.021
b_xmid[13]	1.014	1.022
b_xmid[14]	1.014	1.023
b_xmid[15]	1.003	1.007
b_xmid[16]	1.013	1.022
b_xmid[17]	1.013	1.021
b_xmid[18]	1.011	1.017
b_xmid[19]	1.013	1.021
b_xmid[2]	1.006	1.015
b_xmid[20]	1.017	1.028
b_xmid[3]	1.005	1.015
b_xmid[4]	1.006	1.015
b_xmid[5]	1.006	1.015
b_xmid[6]	1.006	1.015
b_xmid[7]	1.006	1.015
b_xmid[8]	1.006	1.015
b_xmid[9]	1.005	1.013
beta_U_geno	1.001	1.002
beta_U_int	1.001	1.002
beta_U_int_sg	1.001	1.002
beta_U_side	1.001	1.002
beta_xmid_geno	1.009	1.018
beta_xmid_int	1.016	1.025
beta_xmid_int_sg	1.001	1.003
beta_xmid_side	1.001	1.003
deviance	1.002	1.007
interaction_U	1.001	1.002
interaction_xmid	1.001	1.003
L	1.005	1.012
s0	1.002	1.007
side_effect_MU_U	1.001	1.002
side_effect_MU_xmid	1.001	1.003
side_effect_WT_U	1.000	1.000
side_effect_WT_xmid	1.000	1.001
sigma	1.000	1.001
sigma_s	1.001	1.003
sigma_xmid	1.001	1.003

Table 3: Effective sample sizes

Parameter	Effective Sample Size
b_s[1]	7500.4

b_s[10]	7423.2
b_s[11]	5531.5
b_s[12]	6764.3
b_s[13]	5286.2
b_s[14]	6561.5
b_s[15]	2746.6
b_s[16]	7672.9
b_s[17]	6733.2
b_s[18]	6774.3
b_s[19]	7229.8
b_s[2]	6089.0
b_s[20]	4551.6
b_s[3]	6066.3
b_s[4]	6376.0
b_s[5]	6144.5
b_s[6]	5973.8
b_s[7]	7726.3
b_s[8]	4787.1
b_s[9]	7796.1
b_s0	1300.8
b_xmid[1]	248.2
b_xmid[10]	438.3
b_xmid[11]	395.8
b_xmid[12]	431.2
b_xmid[13]	442.1
b_xmid[14]	438.8
b_xmid[15]	1325.0
b_xmid[16]	433.4
b_xmid[17]	427.1

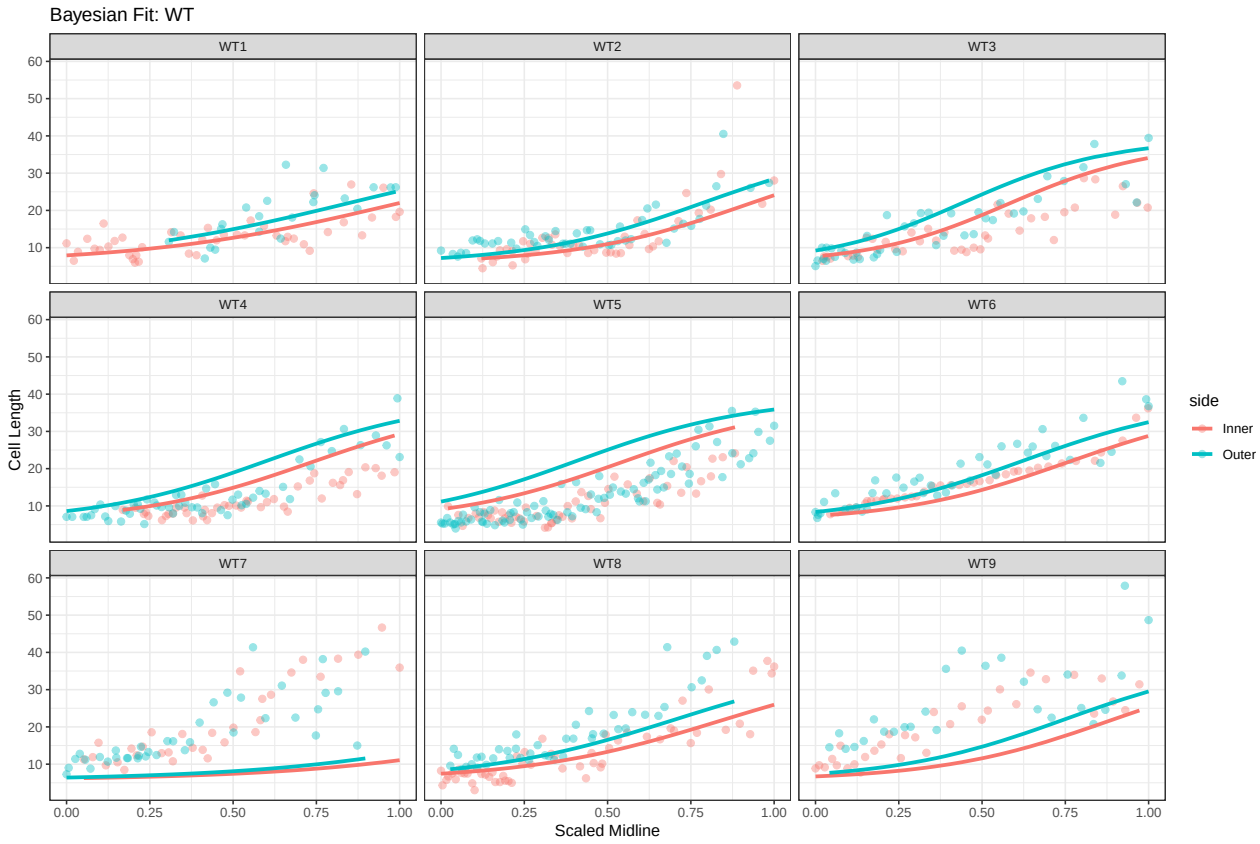

Figure 13: Bayesian fitted curves for WT genotype

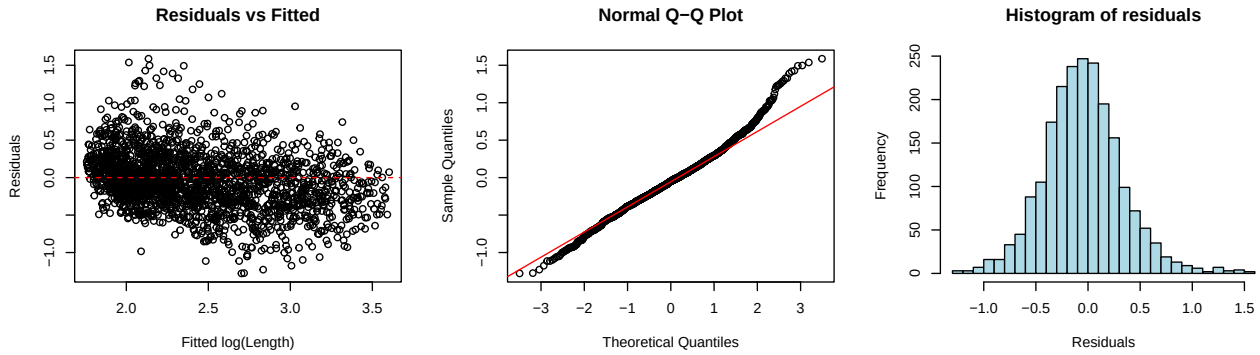

Figure 14: Residuals vs Fitted

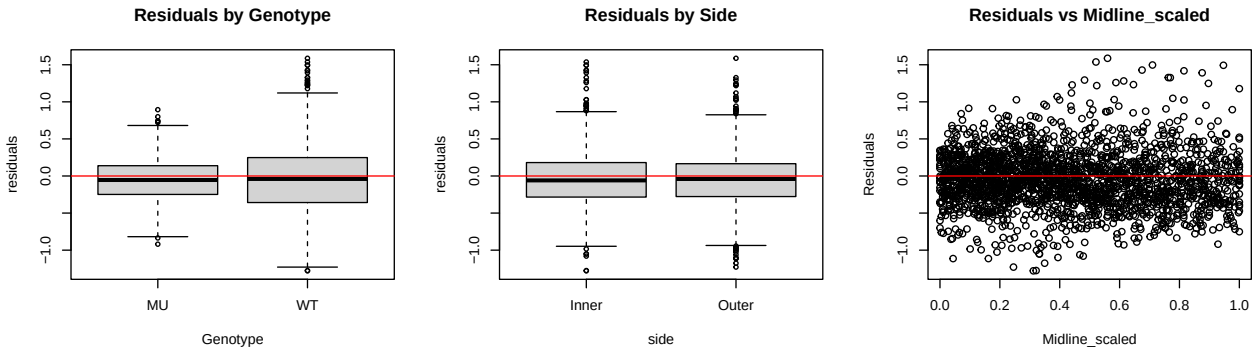

Figure 15: Residuals by grouping variables

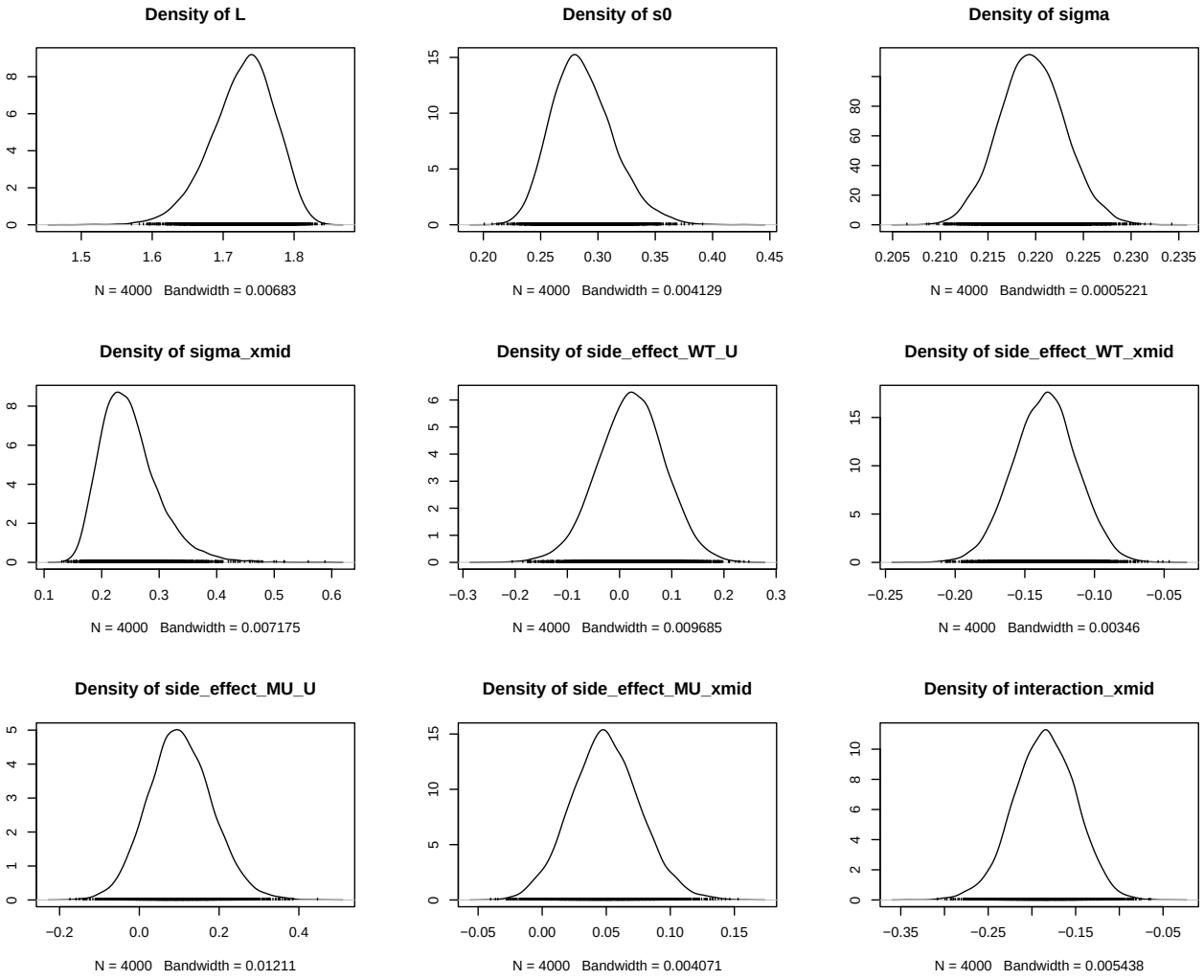

Figure 16: Posterior density plots